Waste Management 108 (2020) 1–12

Contents lists available at ScienceDirect

Waste Management

journal homepage: www.elsevier.com/locate/wasman

Co-composting of sewage sludge and *Phragmites australis* using different insulating strategies

Jiahui Hu [a,b], Zhaohui Yang [a,*], Zhongliang Huang [b], Hui Li [b], Zijian Wu [b], Xuan Zhang [b], Xiaoli Qin [b], Changzhu Li [b], Min Ruan [c], Kang Zhou [b,c], Xikai Wu [b,c], Yanru Zhang [a], Yinping Xiang [a], Jing Huang [b,*]

[a] College of Environmental Science and Engineering, Hunan University, Changsha 410082, PR China
[b] Hunan Academy of Forestry and State Key Laboratory of Utilization of Woody Oil Resource, Changsha 410004, PR China
[c] School of Energy and Power Engineering, Changsha University of Science & Technology, Changsha 410076, PR China

ARTICLE INFO

Article history:
Received 9 January 2020
Revised 16 March 2020
Accepted 7 April 2020

Keywords:
Composting
Laboratory-scale reactor
Temperature
Sewage sludge
Phragmites australis

ABSTRACT

Insulating strategies are indispensable for laboratory-scale composting reactors, however, current insulation methods interfere with the aerobic fermentation behaviors related to composting. To address this issue, a centre-oriented real-time temperature compensation strategy was designed in this study. Five 9 L reactors (R1–R5) with different insulation strategies were used for the co-composting of dewatered sludge and *Phragmites australis* and compared. The process performance was assessed by monitoring the temperature, O_2 and CO_2 emissions, the physical–chemical properties of the composting materials were evaluated by measuring the organic matter (OM), carbon nitrogen ratio (C/N), pH, electrical conductivity (EC), and fluorescence excitation-emission matrix (EEM) spectra. And a 16S rDNA analysis was used to quantify the evolution of bacterial community. The main findings are as follows. Compared with R1 as a control, the insulating strategies can increase the maximum temperature and prolong the thermophilic phase of composting. Comparing R1 and R3 showed that real-time temperature compensation can better restore the real fermentation of the compost. The results showed that R5 had the best composting effect, reaching 69.8 °C, which was 25.1%, 29.7%, 19.3%, and 17.3% higher than R1, R2, R3, and R4, respectively, and remaining in the thermophilic phase for 4.24 d, which is 1.4, 1.5, 1.3, and 0.2 times longer than R1, R2, R3, and R4, respectively. Furthermore, it can significantly reduce the temperature difference between the centre and edge of the reactor, which improved the composting material allocation efficiency and composting process control accuracy, further providing a basis for the actual full-scale composting operation.

1. Introduction

Composting is widely used for converting organic solid wastes into a stable and safe compost that can be reused in agriculture (Meng et al., 2018). The aerobic composting process involves physical, chemical, and biochemical reactions, which are affected by factors such as temperature, particle size, and moisture content (MC). Composting experiments are necessary for determining optimal composting conditions. However, a full-scale composting experiment is expensive, labor intensive, and difficult to control. Thus, laboratory-scale composting reactors, which are easier to operate and can track the composting process, are widely applied.

Laboratory-scale composting results often vary widely due to different equipment and environmental conditions. This is mainly due to the limited amounts of organic substrates and easier heat losses; hence, a rapid drop in temperature is typically observed in small reactors (Petiot and de Guardia, 2004). Therefore, insulating strategies are widely used in laboratory-scale composting reactors.

As shown in Table S1, many laboratory-scale composting reactors (≤100 L) that are commonly used to study the aerobic fermentation behavior of various organic waste materials have been described in the literature. The larger the volume of the composting reactor, the simpler the insulation method needed, such as using polyurethane foam, or mineral wool. With a decrease in composting reactor volume, it becomes more difficult for the reactor to achieve and maintain high-temperature composting conditions

* Corresponding authors at: College of Environmental Science and Engineering, Hunan University, 1 Lushan South Road, Yuelu District, Changsha 410082, PR China (Z. Yang). Hunan Academy of Forestry and State key laboratory of utilization of woody oil resource, No. 658, Shaoshan South Road, Changsha 410004, PR China (J. Huang).

E-mail addresses: yzh@hnu.edu.cn (Z. Yang), gavinhj@163.com (J. Huang).

https://doi.org/10.1016/j.wasman.2020.04.012
0956-053X/

through self-heating. In this case, covering it with insulation material is no longer applicable; most solutions applied to reduce the heat loss from the wall involved placing the reactor in a constant temperature incubator or a water bath for heat losses. However, applying a fixed temperature throughout the entire composting process typically causes artificial conditions, which greatly influence the aerobic fermentation behavior of the organic waste, and even becomes a prerequisite for the start-up and operation of the system, a point which few studies pay attention to. Furthermore, the strong contrast between the temperature inside and versus outside of the compost pile is one of the most challenging aspects of composting. The results from Lau et al. (1992) showed that the vertical gradient between the centre and surface probes (a distance of approximately 30 cm) of the 55 L reactor is greater than 5 °C, (Elwell et al., 1996), indicating that there is a temperature gradient of up to 25 °C between the top and bottom of the 208 L reactor. The temperature difference between the inside and outside of a laboratory-scale composting reactor results in the uneven fermentation of materials and unrepresentative sampling. Hence, it is necessary to improve the consistency between the centre and the edge temperatures in laboratory-scale composting reactors.

In this study, dewatered sludge, an inevitable by-product of the wastewater treatment process (Bai et al., 2018), was selected as the raw material for composting. The dewatered sludge has the characteristics of a high MC (approximately 80%), viscosity, and the low carbon nitrogen ratio (C/N) (Huang et al., 2015), making it unsuitable for composting alone. Therefore, the dewatered sludge should be mixed with dry materials which are rich in carbon, such as sawdust, biochar, wheat straw and green wastes, to adjust the MC and C/N ratio to an appropriate range (Arias et al., 2017). In this study, *Phragmites australis* was used as a bulking agent and carbon source that was mixed with the dewatered sludge for composting, to adjust the MC, C/N ratio, and maintain the air spaces. These raw materials were obtained from the Yanghu wastewater treatment plant located in Changsha, China. The plant has the capacity to treat 120,000 m^3 of domestic wastewater per day, and it adopts the combined treatment technologies of a modified sequencing batch reactor, micro-flocculation filtration, constructed wetland and disinfection. The constructed wetland, spread over 114,136 m^2, is mainly vegetated with *Phragmites australis*, *Typha orientalis*, and *Iris pseudacorus*. These wetland macrophytes will be harvested twice a year, and the annual output of the biomass can reach up to 1500 t. Therefore, the co-composting has provided a potential approach for the sustainable management of the by-products from this plant.

Five kinds of composting reactors (R1–R5) with different insulating strategies were utilized in this study, including one set to room temperature without artificial insulation (R1), one with a thermostat incubator at 30 °C (R2), and three with real-time temperature compensation with maximum heating thresholds of 30 °C, 50 °C, and 70 °C, respectively (R3–R5). The effects of different temperature compensation methods on the reactors were then compared. In summary, the purpose of this study is to design a small compost reactor system with a centre oriented real-time temperature compensation strategy that allows the wall temperature of the reactor to follow the centre temperature of the substrate to achieve more accurate and realistic temperature compensations. The study aims to restore the heat and mass transfer process in the core region of the aerobic fermentation with fewer organic solid wastes, simulate the thermal effects often observed in full-scale composting, and explore the impacts on composting through chemical and biochemical indicators.

2. Materials and methods

2.1. Composting raw materials

A co-composting consisting of sewage sludge and *Phragmites australis* was used for this study. The dewatered sludge was collected after the centrifugal dewatering process, and the *Phragmites australis* was harvested from the constructed wetland in late May, air dried for 2 w, and shredded into pieces of approximately 2 mm. The principal characteristics of the sludge and *Phragmites australis* are listed in Table 1.

The recommended initial MC and C/N ratio at the start of the composting process 50% to 60%, and 20 to 30, respectively. According to these values, the dewatered sludge was mixed mechanically with the shredded *Phragmites australis* at a ratio of 3:2 (w/w), which resulted in a mixture with an initial MC of 58.0 ± 2.2% and C/N ratio of 20.88 ± 0.13.

2.2. Composting reactor and programming

A specially designed composting system was applied to the lab-scale composting process as shown in Fig. 1.

The reactor was a cylindrical vessel made of high density polyethylene (HDPE) with an effective volume of 9 L. The cylindrical vessel was divided into a straw layer and a feedstock layer. Air-dried rice straw was cut to a length of 4–6 cm, it was placed on the top of the feedstock and was approximately 6 cm thick to reduce heat loss and moisture evaporation. A silicone rubber heater of 350 W, which was applied to compensate for the difference in temperature between the centre and edge of the reactor, was wrapped around the reactor. The heater was further insulated by a heat-proof mat to minimize system temperature fluctuations. A micro-porous tube was laid on the bottom of the reactor, and was used to collect the exhaust gas form the composting for analysis. One thermocouple was installed outside the reactor to record ambient temperature changes. Two groups of thermocouples were installed at the centre (Nos. 1 and 2) and edge (Nos. 3 and 4) of the

Table 1
Physicochemical characteristics of the raw material.

Characteristics	Feedstocks			Characteristics	1:20 (w/v) water-extractable		
	Dewatered sludge	*Phragmites australis*	Mixture		Dewatered sludge	*Phragmites communis*	Mixture
Moisture content (wet basis %)	86.5 ± 0.1	22.3 ± 4.9	58.0 ± 2.2	pH	7.05 ± 0.02	6.48 ± 0.1	6.69 ± 0.06
Volatile solid (dry basis %)	57.40 ± 0.07	89.51 ± 0.19	81.62 ± 0.88	EC (mS/cm)	0.52 ± 0.02	2.53 ± 0.46	1.37 ± 0.09
Carbon (dry basis %)	26.98 ± 0.01	45.40 ± 0.04	40.03 ± 0.02	TOC (mg/L)	580.0 ± 1.4	489.8 ± 8.3	358.4 ± 14.2
Nitrogen (dry basis %)	4.71 ± 0.00	1.07 ± 0.04	1.98 ± 0.01	TN (mg/L)	4643 ± 146	3393 ± 203	3737 ± 267
C/N ratio	5.73 ± 0.01	44.87 ± 0.12	20.88 ± 0.13	Protein (mg/mL)	0.055 ± 0.003	0.030 ± 0.005	0.032 ± 0.005
TP (mg/kg)	25306 ± 132	2824 ± 29	7754 ± 59	Polysaccharide (μg/mL)	0.015 ± 0.001	0.030 ± 0.001	0.014 ± 0.004
TK (mg/kg)	6392 ± 307	32952 ± 333	27025 ± 364				
Bulk density (kg/m^3)	1040.4 ± 17.8	82.8 ± 13.2	281.9 ± 16.2				

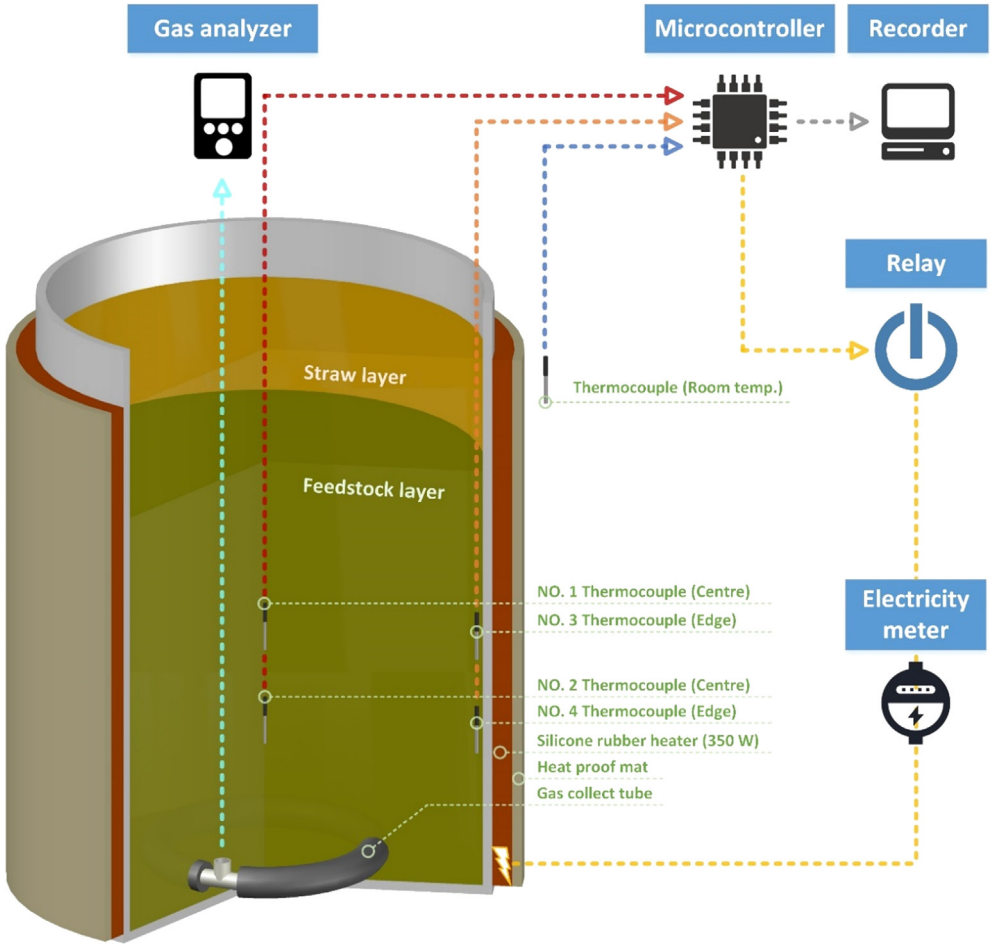

Fig. 1. Schematic of a real-time temperature-controlled compensation reactor for composting.

cylindrical vessel. The temperature was automatically measured every 300 ms, and the average values in each group were the input data for the program-controlled heating. These values were recorded every 15 min to monitor the temperature profiles at the centre and edge of the reactor.

Five reactors (R1–R5) with different insulating strategies were built for the composting process, are shown in Table 2.

R1 was conducted in an indoor environment without specific heating, and provided a control trial for the reactors with artificial heating (R2–R5). In view of the crucial effect of ambient temperature on the initiation of composting, 30 °C was set as an initial point for R2–R5. This moderate insulation phase boosted the microbial activity through a restrained intervention and narrowed the differences in environmental factors among the reactors and the experimental batches. R2 was conducted in a thermostat incubator at a constant 30 °C, which provided a comparison for the reactors with dynamic heating (R3–R5). The programmed logic of dynamic heating in R3–R5 was decided by the numeric comparison of temperatures between the centre and edge of the reactors. The fixed thresholds of R3, R4, and R5 were composed of a high temperature in the centre at 30 °C, 50 °C, and 70 °C, respectively, and a consistent, low temperature at the edge of 30 °C, which was used to select the specific running logic. If the centre temperature is lower than 30 °C, the edge temperature will be kept at 30 °C. If the centre temperature is equal to or greater than 30 °C and lower than the high temperature in the centre, then the edge temperature will be increased using a heater to follow the centre temperature. If the centre temperature is equal to or greater than the high temperature in the centre, then the heater will be stopped.

2.3. Composting experiments

The fully mixed feedstock of dewatered sludge and shredded *Phragmites australis* was divided into five piles with equal weights of 2300 g, which were then inoculated with 10% wt fermented agents acquired in a previous composting process using the same feedstock. The mixture was loosely loaded in the reactors to improve the air distribution. The composting experiment was conducted for 35 d. To maintain the aerobic condition and thermophilic phase for as long as possible, the composting piles were turned manually on days 1, 2, and 3 (D1, D2, and D3), when the centre temperature of the piles had exhibited a decreasing trend. Furthermore, the piles were turned during the cooling phase on Day 7 (D7) and the maturation phase on Day 21 (D21) and Day 35 (D35). All composting reactors were moved to room temperature when the compost entered into the maturation phase on the seventh day.

The sample collected from Day 0 (D0) was the initial compost sample mixed with sludge and *Phragmites australis*. A set of samples (D1, D2, D3, D7, D21, and D35) were collected to represent the mesophilic phase (D0 and D1), thermophilic phase (D1 and D2), cooling phase (D3 and D7), and maturation phase (D21 and D35). The collected solid samples were divided into three parts. One part was immediately used to measure MC and organic matter (OM), and another part was oven-dried at 33 °C for 48 h, after which crushing and sieving (150–300 μm) was used to determine the physicochemical characteristics including pH, electrical conductivity (EC), C/N, dissolved organic matter (DOM), and excitation-emission matrix (EEM). The third part was stored at −80 °C for DNA extraction.

Table 2
Specific instructions for five compost reactors.

Reactors		Temperature thresholds		Running logics
		Centre	Edge	Heater
R1	Room temp.	/	/	/
R2	Constant 30 °C	/	/	/
R3	Dynamic 30 °C	Centre < 30 °C	Edge < 30 °C	ON
			Edge ≥ 30 °C	OFF
		Centre ≥ 30 °C	any	OFF
R4	Dynamic 50 °C	Centre < 30 °C	Edge < 30 °C	ON
			Edge ≥ 30 °C	OFF
		50 °C > Centre ≥ 30 °C	Edge < Centre	ON
			Edge ≥ Centre	OFF
		Centre ≥ 50 °C	any	OFF
R5	Dynamic 70 °C	Centre < 30 °C	Edge < 30 °C	ON
			Edge ≥ 30 °C	OFF
		70 °C > Centre ≥ 30 °C	Edge < Centre	ON
			Edge ≥ Centre	OFF
		Centre ≥ 70 °C	any	OFF

2.4. Analytical methods

2.4.1. Gaseous measurements

The contents of O_2 and CO_2 in the cooled gas bag were determined once per day using a portable biogas analyzer (Gasboard-3200plus, Cubic-Ruiyi, China) equipped with electrochemical and non-dispersive infrared detectors, allowing for the measurement of O_2 (up to 25%) and CO_2 (up to 50%), respectively.

2.4.2. Physicochemical analysis

The MC was determined after oven-drying the fresh samples at 105 °C for 24 h. The dried sample was ignited at 550 °C for 5 h in a muffle furnace to obtain the OM content. The OM loss (OML) was calculated from the initial volatile solids content and the final volatile solids content as follows (Külcü and Yaldiz, 2014):

$$\mathrm{OML}(\%) = \frac{[OM_i(\%) - OM_f(\%)] \times 100}{OM_i(\%) \times [100 - OM_f(\%)]} \quad (1)$$

where OM_i is the initial OM content and OM_f is the final OM content. Elemental compositions of total C and total N in the compost samples were found for the dried samples by catalytic tube combustion using a Vario Macro elemental analyzer (ELEMENTER, Germany). The C:N ratio is the quotient of the total C divided by the total N. Aqueous extracts from the compost samples were prepared with a solid-to-water ratio of 1:20 (w/v, dry weight basis) at 200 r/min for 4 h in a horizontal shaker kept at room temperature. Then the suspension was centrifuged at 12,000 rpm for 5 min, and filtered through a 0.45 μm membrane for the subsequent pH, EC, and EEM determinations. The pH and EC of the aqueous extract were determined using a FE28 pH meter and SevenEasy EC meter (Shanghai, China), respectively.

2.4.3. Fluorescence excitation-emission matrix spectra (EEM) spectra

The concentrations of DOM were measured with a total organic carbon (TOC) analyzer (TOC-V CPH, Shimadzu, Japan). Prior to the fluorescence analysis, the compost extracts were adjusted to DOM < 10 mg/L. The fluorescence EEM spectroscopy was measured with a fluorescence spectrophotometer (F-4600, Hitachi, Japan) in scan mode. Excitation (Ex) and emission (Em) wavelengths were set from 200 nm to 550 nm and 250 nm to 600 nm, respectively, at a sampling interval of 5 nm. The spectra were recorded at a scan rate of 12000 nm/min, the slit width was fixed at 5 nm, and the photomultiplier tube (PMT) voltage was fixed at 700 V. The EEM spectra of distilled water were examined and subtracted from the spectra of the compost-derived DOM.

2.4.4. DNA extraction, polymerase chain reaction (PCR) amplification and sequencing

Due to the ambient temperature being approximately 30 °C, the differences between reactors R1, R2, and R3 were very small, so only the bacterial community of R1, R4, and R5 was tested. Samples were collected on D0, D1, D3, D7, and D35 for reactors R1, R4, and R5. DNA was extracted from the compost samples (0.5 g dried weight) using a Genomic DNA Extraction Kit (Tiangen Biotech, Beijing, China) according to the manufacturer's instructions. The quantity and quality of the extracted DNA were checked by spectrophotometric analysis using the NanoDrop2000 (Thermo Fisher Scientific, USA). Agarose gel electrophoresis confirmed the successful isolation of the DNA. Primers (338F ACTCCTACGGGAGGCAGCAG and 806R GGACTACHVGGGTWTCTAAT) targeting the V3-V4 region of the 16S bacterial rRNA gene were chosen for the amplification and subsequent pyrosequencing of the PCR products (Majorbio Bio-Pharm Technology Co., Shanghai, China). The PCR conditions were as follows: 95 °C for 3 min, followed by 30 cycles at 95 °C for 30 s, 55 °C for 30 s, and 72 °C for 45 s, which was then followed by a final extension at 72 °C for 10 min. The PCR products were purified using a DNA gel extraction kit (Axygen, Tewksbury, MA, USA). A raw sequence analysis was carried out using the Illumina MiSeq paired-end 300 bp protocol (Illumina, Inc., San Diego, CA, USA) at the Majorbio Bio-Pharm Technology Co., Shanghai, China. The quality control procedure for the raw data was performed by USEARCH (Qian et al., 2016) and which used UPARSE to cluster eligible sequences with a similarity level of 97% to form operational taxonomic units (OTUs). All sequencing raw datasets were deposited to NCBI with submission ID SUB6762800.

2.5. Statistical analysis

Data were expressed as the mean ± standard deviation of duplicate measurements (standard deviations are represented as error bars in the figures). Statistical analyses and plots were performed and created using Excel 2007 (Microsoft, USA), OriginPro 8.5 SR1 (OriginLab Corp., USA) and SigmaPlot 12.5 (version 12.5, Systat Software, Inc., USA) software. The analysis of the bacteria community data was conducted using the i-Sanger platform (http://www.i-sanger.com/).

3. Results and discussion

3.1. Changes in composting temperature

Temperature is a key predisposing factor that affects the rate of microbial activity and degradation during aerobic composting

(Zhang et al., 2015). Temperature changes in the centre of the compost (C) and in the edge of the compost (M) during the 35 days of composting in the five composting reactors R1–R5 are presented in Fig. 2(a–e).

Reactors R1–R5 all operated normally according to the respective set conditions and procedures. Similar to the traditional composting process, the five reactors experienced four phases: the mesophilic phase (15–45 °C), thermophilic phase (>45 °C), cooling phase (<45 °C), and maturation phase (at room temperature) (Cui et al., 2017; Van der Wurff et al., 2016). The temperature of the five reactors increased rapidly without any lag phases in the mesophilic phase and reached the thermophilic phase (>45 °C) during the first day. An increased temperature indicated that intense microbial activity had occurred and thermophilic microorganisms had rapidly multiplied, producing large amounts of heat and gas by decomposing into easily degradable OM, such as glucose and other carbohydrates, leading to an increase in composting temperature (Liu and Wang, 2018). Then, with the consumption of the easily decomposable substances, the temperature gradually decreased (except for R5, which continued to maintain at a temperature of approximately 66 °C). After the first turning, the thermophilic aerobic microorganisms reproduced due to the replenishment of moisture and oxygen, and the decomposable cellulose macromolecules slowly began to be consumed. Therefore, the temperature of R1–R5 rebounded, After the second turning and water replenishing, the temperature of the five reactors still showed a downward trend until they reached the ambient temperature, indicating their gradual entering into the maturation phase after the cooling phase.

As the ambient temperature of composting at that time was approximately 30 °C, which was similar to the set temperature of the thermostat incubator, the temperature of R2 was not greater than R1. Meanwhile, although the maximum heating threshold of reactor R3 was also set at 30 °C, the temperature change in R3 was similar to that in R1, and it reached a higher temperature and endured a longer thermophilic phase, indicating that centre oriented real-time temperature compensation can better restore the real fermentation situation of compost and improve the composting effect. To clearly show the temperature difference between the five reactors, the maximum temperature reached in each reactor was recorded daily as shown in Fig. 2f. The temperature cumulation (TC, °C·d) index was defined by Zhang et al. (2008) as the sum of the temperature difference between the daily average waste and environmental temperatures based on the following equation and as shown in Fig. 2g

$$TC = \sum_{i=1}^{n} (T_m - T_a) \cdot \Delta t \quad (2)$$

where T_m (°C) and T_a (°C) are the waste temperature and environmental temperature at day i respectively, and Δt is the time element (1d). The maximum temperatures achieved in reactors R1–R5 were 55.8 °C, 53.8 °C, 58.5 °C, 59.5 °C, and 69.8 °C, respectively. Like in the typical green waste composting process, due to the high OM content, the thermophilic phase begins in the first two days of composting, but the duration is relatively short (less than 4 d) (Reyes-Torres et al., 2018). The duration of the thermophilic phase in reactors R1–R5 were 1.77d, 1.67d, 1.83d, 3.53d, 4.24 d. In general, the centre-oriented real-time temperature compensation strategy is helpful increasing the maximum temperature and prolonging the thermophilic phase, especially for reactor R5 (maximum heating threshold is set at 70 °C), which reached 69.8 °C and the thermophilic phase was maintained for 4.24 days, which was high and long enough to maximise sanitation and destroy pathogens (Petric et al., 2009). In contrast, the reactor with centre-oriented real-time temperature compensation reduced the temperature difference between the centre and the edge of the composting pile. In particular, the temperature changes in the centre and the edge of the reactor R5 were essentially the same.

As shown in Fig. 2h, reactors R3-R5, which all used a centre oriented real-time temperature compensation strategy, recorded the daily electricity consumption of the reactor in the first six days. Reactor R3, due to the maximum heating threshold being set to 30 °C, which was similar to the room temperature during the composting process in this study, the electricity consumption was far less than the recording range of electricity, where the electricity consumption is displayed as 0. The daily electricity consumption of reactors R4 and R5 was positively correlated with temperature, and there was very little electricity consumption, which indirectly indicates that the reactor is operating normally.

3.2. Evolution of CO_2 and O_2 concentrations

During composting, microorganisms use carbon sources to consume oxygen and produce CO_2. The O_2 concentration is one of the decisive factors of oxygenic decomposition, and it is directly related to the self-heating characteristics of compost and other gas emissions (Czekała et al., 2016). The main gas produced by microorganisms for OM degradation is CO_2, which is directly related to the respiratory chain, reflecting the degradation of OM and microbial activity during composting (Wu et al., 2015). Therefore, the rate of O_2 consumption and CO_2 production during composting indicates the degree of decomposition of OM and the extent of the composting reaction, respectively. At the beginning of the experiment, the O_2 content in each reactor was approximately 20.7%, which was equivalent to the content in the atmosphere (Fig. 3a) and the CO_2 content was approximately 0.09% (Fig. 3b).

On the first day of composting, the O_2 content of each reactor decreased rapidly and reached its lowest value, and the corresponding increase in CO_2, was similar to the results reported in some literature (Yuan et al., 2016). In addition, the peak levels of reactors R3, R4, and R5 were comparable, while R1 and R2 were generally lower. This is likely due to the high content of easily decomposed OM in the early stage of composting that was rapidly utilized by microorganisms, gradually increasing the microbial activity and resulting in a great amount of oxygen consumption and a sharp increase in the production of CO_2. This also led to an increase in temperature and the rapid entering into thermophilic phase, indicating that the centre oriented real-time temperature compensation strategy can quickly activate microbial activity in a small composting reactor.

Following the initial drop, the O_2 content in each reactor began to rise on the second day until it stabilized at approximately 20.2%. In contrast, after the initial rise, the CO_2 content in each reactor began to decline on the second day until it stabilized at approximately 0.7%. This is probably due to the thermal inhibition of microbial activity and the reduction in readily soluble nutrients. During this period, a small peak occurred at the same time from the 5th day to 10th day for reactors R1 and R3, which corresponded to a rise in the reactor temperatures. Additionally, except for the difference in peak values in the high-temperature period on the first day, the gas distributions of R1 and R3 were consistent, while R2, being under a constant temperature environment, presented another type of peak shape. These results indicated that real-time temperature compensation can minimize the effects of external environmental conditions on the reactor and obtain a more accurate fermentation state of the reactor. The O_2 and CO_2 contents both tended to be stable after 11 d, indicating that the compost gradually reached stabilization and maturation.

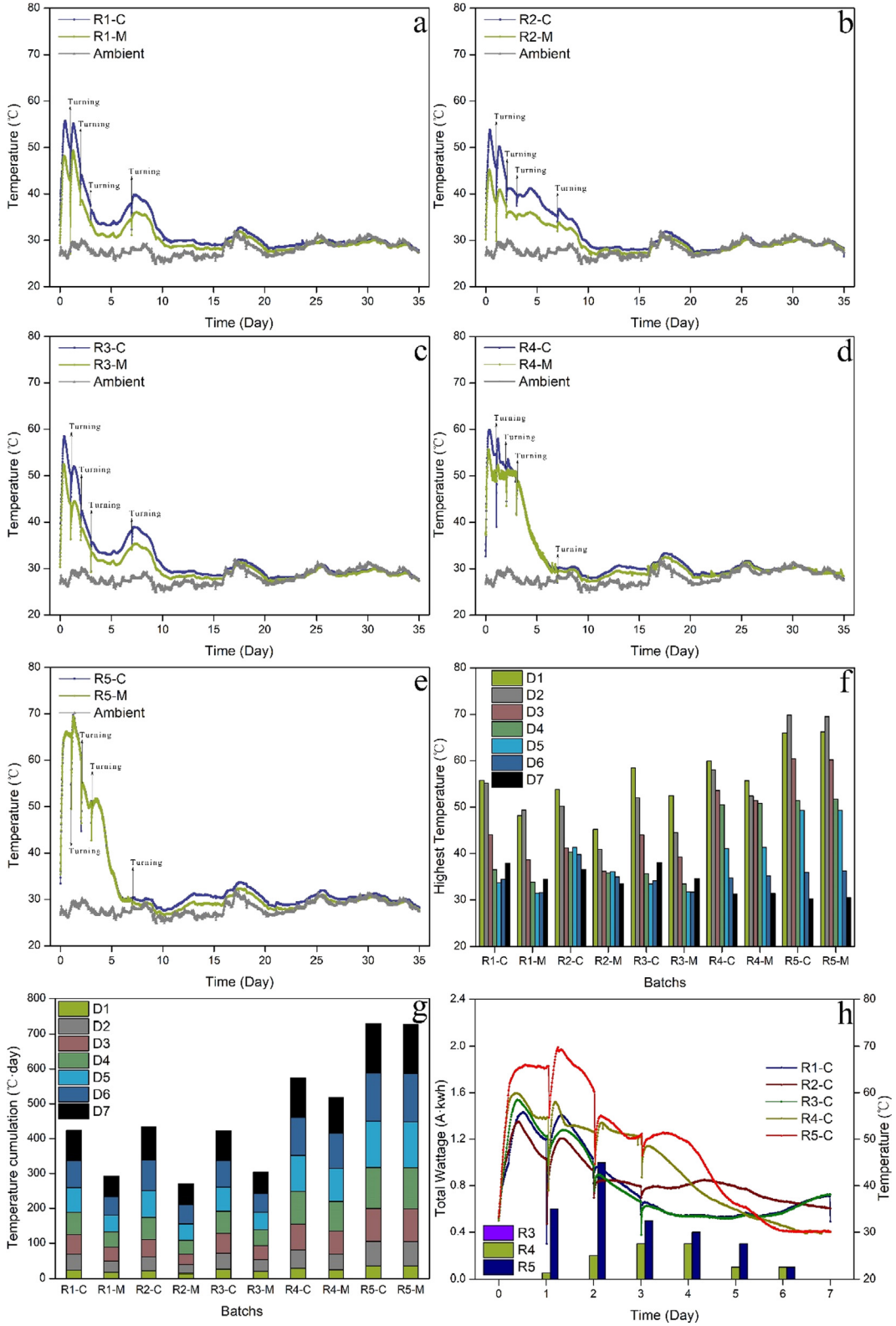

Fig. 2. (a–e) Temperature changes in the centre of the compost (C) and in the edge of the compost (M) during the 35 days of composting in the composting reactors R1–R5. (f–g) Daily maximum compost temperature records and cumulative temperatures in the centre (C) and edge (M) of five reactors R1–R5 in the first 7 days. (h) Temperature changes in the centre of the compost (C) during the first 7 days of composting in the composting reactors R1–R5, and records of daily electricity consumption during the first 6 days of composting in the composting reactors R3–R5.

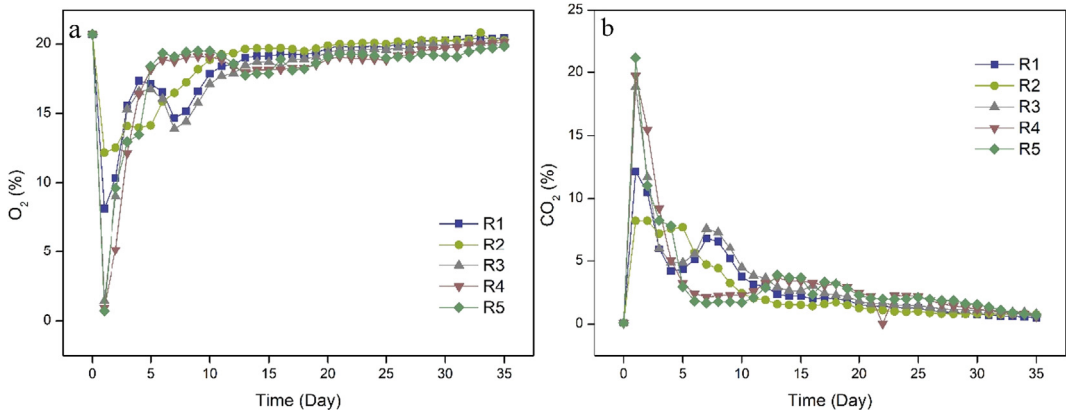

Fig. 3. Evolution of the concentrations of (a) O_2 and (b) CO_2 in the outlet gas flow during the 35 days of composting in each reactor.

3.3. Organic matter biodegradation and C/N evolution

The degradation of OM is a well-known and valuable index for evaluating composting effectiveness (Wang et al., 2016). As expected, the OM content decreased during the composting process in all reactors (Fig. 4a)

The OM contents in R1, R2, R3, R4, and R5 decreased from the original 81.62% to 72.70%, 72.72%, 74.68%, 72.77%, and 72.17%, respectively, within 35 d. Based on these results, to quantify the mineralization of organic matter, the OML over time during composting was calculated as 11.01%, 10.98%, 8.57%, 10.92%, and 11.66%, for R1, R2, R3, R4, and R5, respectively. The OML values of the five reactors were not significantly different, and the degradation degree of the R5 reactor was slightly higher than that of other reactors.

The C/N ratio is another valuable indicator reflecting compost maturity and stability (Awasthi et al., 2014). Similar to OM, the C/N ratio of all reactors also exhibited a downward trend, as presented in Fig. 4b. The C/N ratio in all reactors decreased from 20.88 on D0 to the following final values on D35: 10.85 (R1), 11.02 (R2), 11.22 (R3), 11.05 (R4), and 11.32 (R5). The decrease in the C/N ratio is most likely due to microbial respiration (Bernai et al., 1998). According to Heerden et al. (2002), a C/N ratio of less than 20 indicates that the compost is mature, and a relatively strict C/N ratio for agriculture needs to be less than 15. Jimenz and Garcia (1992) proposed that a C/N ratio of less than

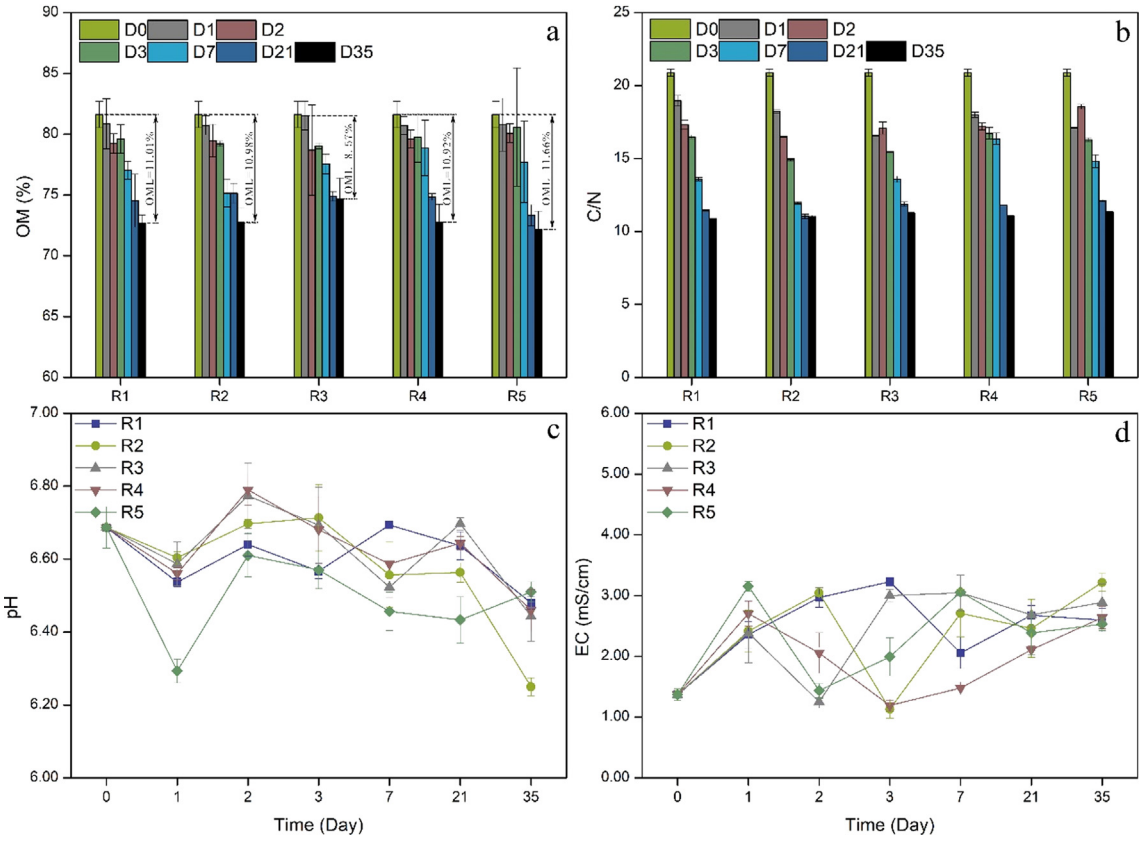

Fig. 4. (a) OM, (b) C/N, (c) pH, and (d) EC evolution in the five reactors during the composting process. The error bars represent the standard deviation.

12 indicates that the Green waste compost is mature. Some studies have suggested that the C/N values of different composting materials used to indicate composting maturity are different, and it varies greatly depending on the initial materials; therefore, the C/N ratio cannot be used as an absolute indicator of composting maturity (Cofie et al., 2009; Guo et al., 2012). It is therefore recommended to use a T value (T = the final C/N ratio/the initial C/N ratio) to evaluate the degree of maturity (T < 0.6 indicates mature compost) (Chen et al., 2018). In the current study, the T values of reactors R1–R5 were 0.52, 0.53, 0.54, 0.53, and 0.54, respectively, all consistent with the T < 0.6 threshold, indicating that compost in all reactors had reached maturity.

3.4. Variation in pH and electrical conductivity

The appropriate pH range for composting is 5.5–8.5 (Karak et al., 2014), which is within the range of the compost in this study. Fig. 4c shows the variation in pH with composting time for the five reactors. The pH for R1, R2, R3, R4, and R5 decreased from the initial 6.69 to the minimum 6.54, 6.60, 6.59, 6.29, and 6.29 on D1, respectively, followed by a fluctuation and a gradual decrease until the end of the composting process. The decrease in pH in the first day may be due to the volatilization of ammoniacal nitrogen, hydrogen ions released by microbial nitrification, release of CO_2 and formation of organic and inorganic acids in the OM degradation process (Eklind and Kirchmann, 2000; Mathur, 1991). Subsequently, the pH gradually rose, which can be explained by the disappearance of organic acids (such as acetic acid and butyric acid) that were formed in the first stage and the ammonification of organic nitrogen by the microbial biomass with the release of hydroxyl ions and ammonium (Said-Pullicino et al., 2007). In the later stage of maturation, the decrease in pH may be related to ammonia volatilization.

The EC reflects the salinity of the compost product, indicating its possible phytotoxic/phyto-inhibitory effects on plants (e.g., low germination rate, withering) if used as a fertilizer (Chitsan, 2008). As shown in Fig. 4d, EC values generally increased during the process in all reactors. The EC values for R1, R2, R3, R4, and R5 increased from the initial value of 1.37 mS/cm on D0 to 2.60 mS/cm, 3.22 mS/cm, 2.89 mS/cm, 2.64 mS/cm, and 2.53 mS/cm on D35, respectively. Bertran et al. (2004) attributed the increase in EC to the mineralization of the compost materials. It may also be related to water evaporation and concentration increase from the composting process or the release of soluble salts (e.g., ammonium and phosphate) from the biodegradable organic decomposition after the active phase (Rawat and Suthar, 2014). Awasthi et al. (2014) mentioned that an EC value greater than 4 mS/cm will adversely influence plant growth, and the EC values in this study were all in the range of 1.19–3.22 mS/cm, which satisfies the requirement of compost maturity and safety.

3.5. Fluorescence excitation-emission matrix spectra analysis

Composting is an OM humification process (He et al., 2011), and the humic substances produced are fluorescent compounds. Therefore, the EEM fluorescence spectra is widely used to evaluate the quality of the humic substances and maturity of the compost. Compared with the typical physical–chemical method, the EEM fluorescence spectra can save time, and the requirements of sample pretreatment are very low (Tang et al., 2011). The EEM fluorescence spectra was divided into five regions depending on the wavelengths of the organics according to the protocol of Chen et al. (2003). The EEM spectra of the DOM extracted from the dewatered sludge (Fig. 5a) and *Phragmites australis* (Fig. 5b) exhibited only two fluorophores, one of which (peak A) was located in region I and II, and the other (peak B) in region IV, indicating that large amounts of simple aromatic proteins and soluble microbial byproduct-like material was present in the raw materials.

The fluorescence intensity of sludge was significantly higher than that of *Phragmites australis*. At the beginning of composting (D0), there were also two fluorophores which were consistent with the raw materials (Fig. 5c), i.e. the positions of peak A (Ex/Em = 227–231 nm/318–338 nm) and peak B (Ex/Em = 274–283 nm/335–345 nm). This suggests that the simple aromatic proteins and soluble microbial byproduct-like materials were the dominating portion of the DOM in the aqueous extraction of the initial mixed compost sample. After 35 d of composting, the

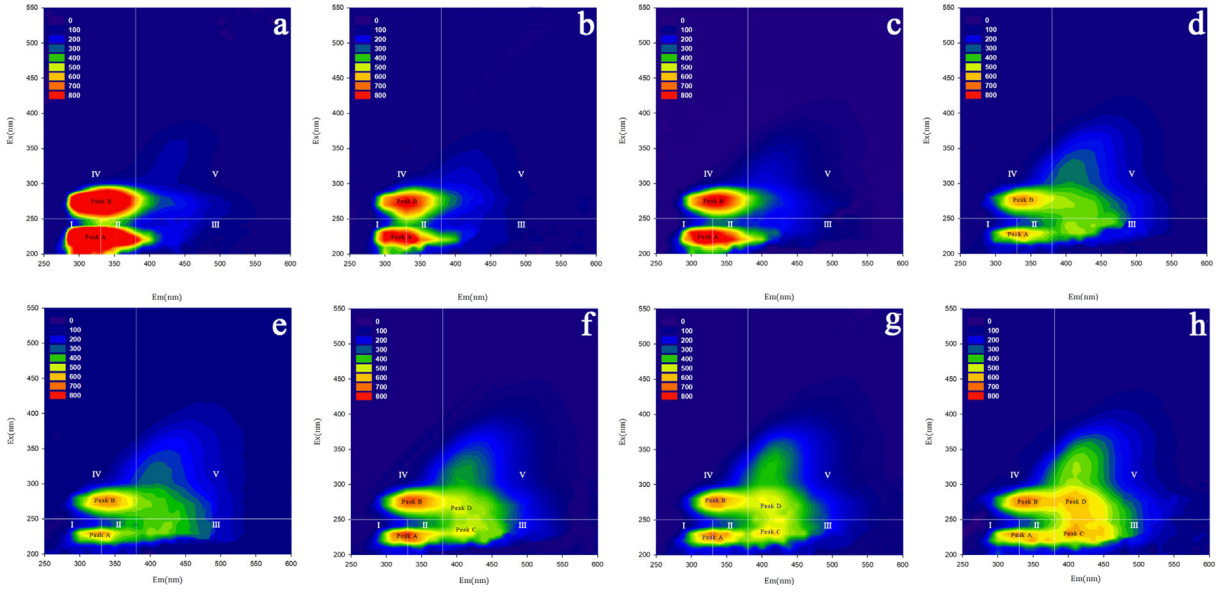

Fig. 5. EEM spectra of: (a) primary sludge, (b) *Phragmites australis*, (c) composting sample at D0, and (d)-(h) composting samples on D35 for reactors R1–R5. The white lines divide the EEMs into regions (I–V): Region I and II are related to simple aromatic proteins (Region I: Ex: < 250 nm, Em: < 330 nm, tyrosine-like organic compounds; Region II: Ex: < 250 nm, Em:330–380 nm, tryptophan-like organic compounds), region IV (Ex: 250–280 nm, Em: < 380 nm) is related to soluble microbial byproduct-like materials, and region III (Ex: < 250 nm, Em: > 380 nm) and V (Ex: > 250 nm, Em: > 380 nm) are related to fulvic acid-like materials and humic acid-like materials, respectively.

fluorescence intensity of peaks A and B in the five reactors decreased and showed a trend of moving toward the right (regions III and V) (Zhang et al., 2014), because of the degradation of OM caused by microbial activity (He et al., 2011). The change of EEM indicates that the easily-degradable organic matter components (such as polysaccharides, aliphatic chains, and protein) had decomposed and the improvement of humus level. A lack of humification material was observed in reactors R1 and R2 through peaks C and D which indicated that the humic acid-like and fulvic acid-like materials were nearly invisible (Fig. 5d and e). Peak C and D appeared in reactors R3, R4, and R5 (Fig. 5(f–h)). The fluorescence intensities of peak C (Ex/Em = 228–233 nm/415–422 nm) and peak D (Ex/Em = 269–273 nm/395–402 nm) in reactor R3 were weak, and the peaks were not obvious. In contrast, the fluorescence intensities of peak C (Ex/Em = 228–232 nm/415–422 nm) and peak D (Ex/Em = 267–283 nm/393–415 nm) in reactor R4 were slightly stronger than those in reactor R3. Peak C (Ex/Em = 226–234 nm/397–407 nm) and D (Ex/Em = 271–283 nm/389–410 nm) in reactor R5 were the most clearest, and the fluorescence intensities were the strongest. In conclusion, reactors using a centre-oriented real-time temperature compensation strategy were more conducive to compost maturity, especially in the reactor R5 with its maximum heating threshold set to 70 °C.

3.6. Bacterial community

3.6.1. The diversity of the bacterial community

Through clustering, a statistical analysis of biological information was performed on the OTU at a 97% similarity level. The Shannon and Simpson indices were calculated to present the bacterial community diversity, a higher Shannon or lower Simpson value indicated higher community diversity (Liu et al., 2018). As shown in Table S2, the high coverage value indicates that the results are credible. The OTU numbers and the Chao 1, Ace, Shannon, and inverse Simpson indices showed that the highest community richness and diversity were found on D0, and the bacterial richness and diversity decreased after the temperature of reactors increased on D1, indicating that the high temperature of the reactor during the composting altered the microbial communities (Cai et al., 2016). The microbial richness decreased after exposure to high temperatures. Overall, due to the high temperature, the richness and diversity of the compost bacterial community were significantly reduced; they recovered after the cooling phase but still far less than the initial composting period (D0) values.

According to the principal coordinates analysis (PCoA) based on the Bray-Curtis distance, PC1 and PC2 accounted for 62.33% of the total variation (Fig. 6a).

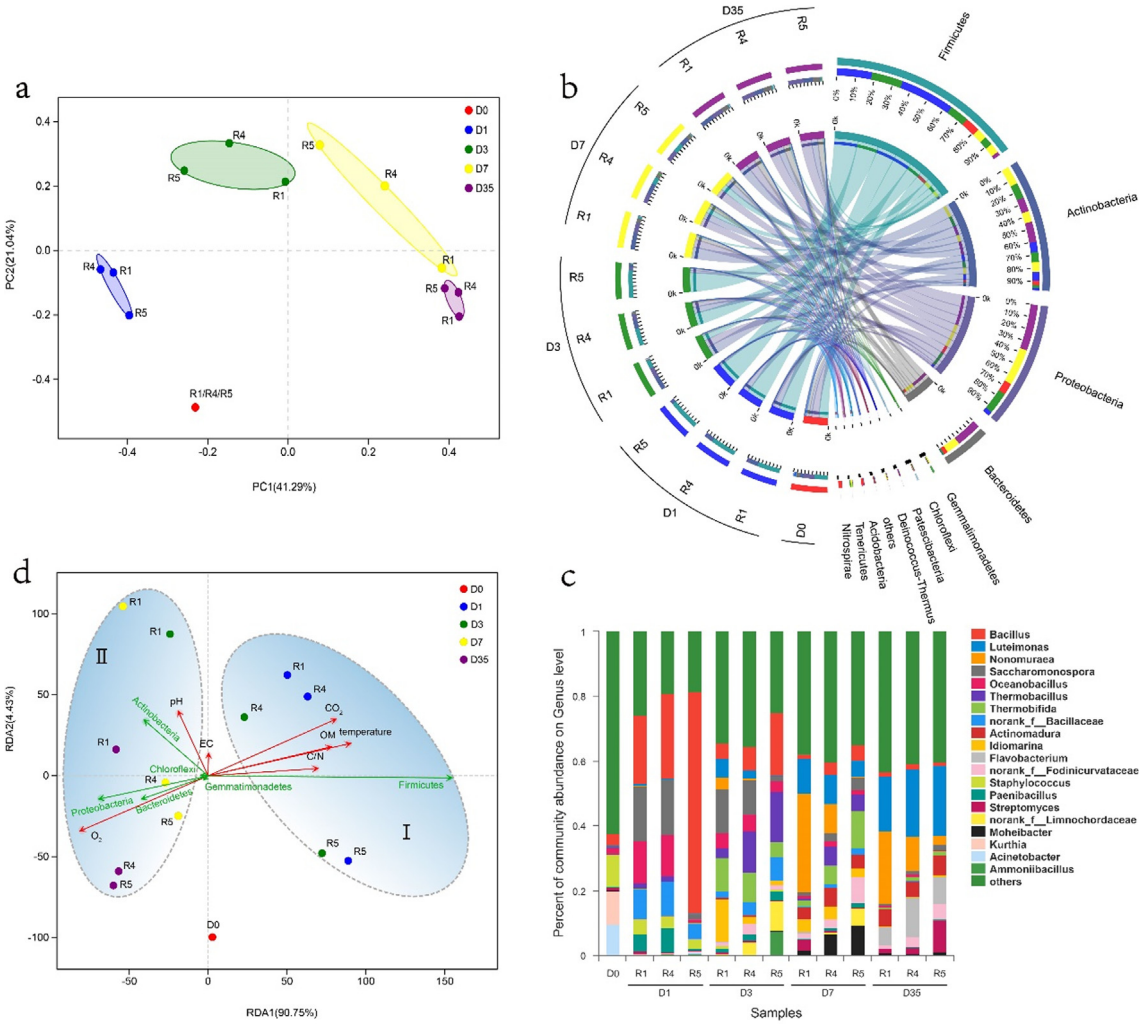

Fig. 6. Bacterial community analyses conducted during composting. (a) PCoA of the bacterial communities in the compost based on OTUs. (b) Distribution of bacterial community for each composting reactor at the Phylum level that was visualised by Circos. (c) Genus level composition of the bacteria community. (d) Redundancy analysis (RDA) assessing the relationship between environmental factors (red arrows) and main bacterial communities (green arrows) at the phylum level.

It can be seen from Fig. 6a that the community structure of the compost was divided into four distinct profiles corresponding to distinct phases of composting, proving that composting periods play a significant role in shaping the bacterial community, which has also been shown in previous studies (Zhang et al., 2016). In contrast, the community difference of each reactor increased at first, but after further compost maturation, the differences in the compost diminished significantly, indicating that the compost tended to be stable.

3.6.2. The structure of the bacterial community

The Circos graph can be used to represent the proportion of different species in each sample and the proportion of the same species in different samples; the width of the bars indicate the relative abundance of that phylum in the sample. The composition of the dominant species throughout the entire composting process were similar for three reactors: *Firmicutes*, *Actinobacteria*, *Proteobacteria*, and *Bacteroidetes* were the four main dominant phyla as shown in Fig. 6b, accounting for over 95% of the total bacterial 16S rRNA gene sequences. The composting materials of three reactors, R1, R4, and R5, at D0 were all rich in *Firmicutes* (38.54%), *Actinobacteria* (11.27%), *Proteobacteria* (30.43%), and *Bacteroidetes* (10.68%). The relative abundance of bacterial communities at the phylum level was different based on composting time. On D1, the relative abundances of the *Firmicutes* in reactors R1, R4, and R5 increased significantly (to 65.79%, 73.13%, 89.49%, respectively), becoming the dominant bacteria. Studies have shown that *Firmicutes* can survive at high temperatures (>55 °C), and they were prevalent in the mesophilic and the thermophilic phases (Yin et al., 2017). In addition to having the ability to hydrolyze sugar and protein to produce various acids, lipids, and alcohols (Zverlov et al., 1998), the bacteria in the *Firmicutes* phylum are reported to play a specific role in promoting cellulose degradation and utilisation (Pandey et al., 2013), and many *Firmicutes* can produce endospores to resist dehydration and extreme environments (Xi et al., 2015; Xu et al., 2017). In this study, reactors R4 and R5, especially R5, showed significantly more *Firmicutes*, which may be because the reactor which used a centre oriented real-time temperature compensation strategy contributed the greatest to the compost heating, improving the activity of the bacteria in the *Firmicutes* phylum and contributing to the degradation of OM and accelerated maturation. After the first day of composting, the relative abundances of the *Firmicutes* were reduced, while the *Actinobacteria*, *Proteobacteria*, and *Bacteroidetes* increased. *Actinobacteria* and *Proteobacteria* are the dominant communities in the cooling and maturation phases and can inhibit pathogenic microorganisms by producing various antibiotics, thereby reducing the biotoxicity of compost products (Qian et al., 2016). *Bacteroidetes* is a bacterial community that specialises in degrading high molecular weight compounds. At D35, *Actinobacteria* (36.61%, 26.43%, and 26.38%, respectively), *Proteobacteria* (35.52%, 38.86%, and 44.45%), and *Bacteroidetes* (21.75%, 25.19%, and 23.11%) became the dominant bacteria for R1, R4, and R5, recpectively, and the community differences between the reactors decreased, indicating that the bacterial community structure tended to be stable by the end of composting.

The relative percentages at the genus level are shown in Fig. 6c. Species with an abundance of less than 0.05 in all samples were classified as others. On the first day of composting, the dominant genera included *Bacillus*, *Oceanobacillus*, *norank_f_Bacillaceae*, and *Saccharomonospora*. Among them, *Bacillus*, *Oceanobacillus*, and *norank_f_Bacillaceae* all belong to *Firmicutes*, which is consistent with the results show in Fig. 6b. In particular, the abundance of *Bacillus* in reactor R5 was very high, 68.4%, while those in R1 and R4 were 21.16% and 26.25%, respectively. *Bacillus* is resistant to high temperatures and produces spores with a special resistance to adverse conditions. On the third day of composting, the main genera of R1 were *Saccharomonospora* (13.65%), *Thermobifida* (10.23%), and *Idiomarina* (13.08%); the main genera of R4 were *Saccharomonospora* (10.45%), *Thermobacillus* (12.80%), and *Thermobifida* (8.75%); and the main genera of R5 were *Bacillus* (19.38%), *Thermobacillus* (15.52%), and *norank_f_Limnochordaceae* (9.46%), from which it can be found that the dominant bacteria in reactors R4 and R5 were still *Firmicutes*, while R1 were *Actinobacteria*. After seven days of composting, the main bacterial species in the three reactors were different at the genus level, but all belonged to *Actinobacteria*, *Proteobacteria*, and *Bacteroidetes*, corresponding to the results in Fig. 6b, and indicating that they were the dominant bacteria in the late stages of composting, which was also consistent with previous studies (Mao et al., 2018). At the end of the composting process, the bacterial community composition is essentially the same among the reactors; the main genera of R1 were *Nonomuraea* (22.31%), *Luteimonas* (16.92%), and *Flavobacterium* (5.46%); the main genera of R4 were *Luteimonas* (20.82%), *Nonomuraea* (10.75%), *Flavobacterium* (12.02%), the main genera of R5 were *Luteimonas* (21.45%), *Streptomyces* (9.78%), and *Flavobacterium* (8.16%). *Streptomyces* is one of the dominant genera in R5, belonging to *Firmicutes*, and its abundance is lower in R1 (1.32%) and R4 (1.96%), showing that R5 has a great influence on *Firmicutes*.

3.6.3. The relationship between environmental parameters and the bacterial community

Redundancy analyses were carried out to assess the relationship between the physical–chemical parameters of the compost (temperature, CO_2, O_2 OM, C/N, pH, and EC) and bacterial communities to clarify the extent of the influence of environmental parameters on bacterial community composition and which parameters were most influential, RDA1 and RDA2 explained 95.18% of the total variation (Fig. 6d). Among all environmental parameters, temperature ($P = 0.001$), CO_2 ($P = 0.001$), O_2 ($P = 0.001$), OM ($P = 0.006$), and C/N ($P = 0.033$) had the greatest impacts on driving the succession of bacterial species, demonstrating an extremely significant correlation. The research report of Cahyani et al. (2003) indicated that the temperature of the pile and the substrate available to the bacteria are two main factors driving the succession of a bacterial community. The research of Zhang et al. (2011) also mentioned that the metabolism of microorganisms is highly dependent on temperature, and the dynamics of microbial community composition is strongly influenced by temperature. The content of oxygen in the reactor determines the species of microorganisms and affects the population and activity of the microbes of the composting reactor; therefore, it has an important impact on the temperature of the reactor. The OM value and C/N ratio are associated with the carbon and nitrogen sources for microbes, which are an important parameters in reflecting the process of OM degradation and compost maturity (Huang et al., 2017). According to the distribution of sample points, the process can be roughly divided into two parts (Part I: early stage of composting and Part II: late stage of composting). Based on the location of the sample points and green arrows in Fig. 6d, *Firmicutes* was mainly distributed in the mesophilic and thermophilic phases (Part I), as confirmed with the variation in the bacterial community structure (Fig. 6b), and it was positively correlated with pile temperature, CO_2, OM and C/N, while *Proteobacteria*, *Actinobacteria*, and *Bacteroidetes* were mainly distributed in the cooling and maturation phases (Part II) and were positively correlated with O_2. Therefore, it can be inferred that temperature, OM, and C/N were the main factors affecting the bacterial activity (mainly *Firmicutes*) in the thermophilic phase, and the results prove that there was an important relationship between O_2, CO_2, and the dynamics of the bacterial community.

4. Conclusions

The results show that thermal insulation strategies had a significant effect on composting behavior, the centre oriented real-time temperature compensation can increase the maximum temperature, prolong the thermophilic phase of composting, better restore the real fermentation of the compost, and improve the consistency between the centre and edge temperature. Due to the reactor R5 reached maximum temperature, the quantity and activity of *Bacillus* were increased significantly which accelerated the degradation of organic matter and reached the highest degree of humification. These results contribute to the laboratory composting research and provide more stable and reliable basic data and technological support for the actual operation of aerobic fermentation systems.

Declaration of Competing Interest

The authors declare that they have no known competing financial interests or personal relationships that could have appeared to influence the work reported in this paper.

Acknowledgments

This work was supported by the National Natural Science Foundation of China (51808216, 51878258, 51608052), China Postdoctoral Science Foundation funded project (2018M640752), Science and Technology Planning Project of Hunan Province, China (2019JJ50665, 2018RS3109), National Key Research and Development Project (2017YFC0505505), Science and Technology International Cooperation Project of Changsha City (KQ1907082, KQ1801027), Training Program for Excellent Young Innovators of Changsha (KQ1802010, KQ1802040).

Appendix A. Supplementary material

Supplementary data to this article can be found online at https://doi.org/10.1016/j.wasman.2020.04.012.

References

Arias, O., Vina, S., Uzal, M., Soto, M., 2017. Composting of pig manure and forest green waste amended with industrial sludge. Sci. Total Environ. 586, 1228–1236. https://doi.org/10.1016/j.scitotenv.2017.02.118.

Awasthi, M.K., Pandey, A.K., Khan, J., Bundela, P.S., Wong, J.W.C., Selvam, A., 2014. Evaluation of thermophilic fungal consortium for organic municipal solid waste composting. Bioresour. Technol. 168, 214–221. https://doi.org/10.1016/j.biortech.2014.01.048.

Bai, Y., Xu, R., Wang, Q.-P., Zhang, Y.-R., Yang, Z.-H., 2018. Sludge anaerobic digestion with high concentrations of tetracyclines and sulfonamides: Dynamics of microbial communities and change of antibiotic resistance genes. Bioresour. Technol. 276, 51–59. https://doi.org/10.1016/j.biortech.2018.12.066.

Bernai, M.P., Paredes, C., Sánchez-Monedero, M.A., Cegarra, J., 1998. Maturity and stability parameters of composts prepared with a wide range of organic wastes. Bioresour. Technol. 63 (1), 91–99. https://doi.org/10.1016/S0960-8524(97)00084-9.

Bertran, M., Soliva, M., Trillas, I., 2004. Composting winery waste: sludges and grape stalks. Bioresour. Technol. 95 (2), 203–208. https://doi.org/10.1016/j.biortech.2003.07.012.

Cahyani, V.R., Matsuya, K., Asakawa, S., Kimura, M., 2003. Succession and phylogenetic composition of bacterial communities responsible for the composting process of rice straw estimated by PCR-DGGE analysis. Soil Sci. Plant Nut. 49, 619–630. https://doi.org/10.1080/00380768.2003.10410052.

Cai, L., Chen, T.B., Gao, D., Yu, J., 2016. Bacterial communities and their association with the bio-drying of sewage sludge. Water Res. 90 (90), 44–51. https://doi.org/10.1016/j.watres.2015.12.026.

Chen, H., Dou, J., Xu, H., 2018. Remediation of Cr(VI)-contaminated soil with co-composting of three different biomass solid wastes. J. Soils Sedm. 18 (3), 897–905. https://doi.org/10.1007/s11368-017-1811-4.

Chen, W., Westerhoff, P., Leenheer, J.A., Booksh, K., 2003. Fluorescence Excitation−Emission Matrix Regional Integration to Quantify Spectra for Dissolved Organic. Matter. Environ. Sci. Technol. 37 (24), 5701–5710. https://doi.org/10.1021/es034354c.

Chitsan, L., 2008. A negative-pressure aeration system for composting food wastes. Bioresour. Technol. 99 (16), 7651–7656. https://doi.org/10.1016/j.biortech.2008.01.078.

Cofie, O., Kone, D., Rothenberger, S., Moser, D., Zubruegg, C., 2009. Co-composting of faecal sludge and organic solid waste for agriculture: Process dynamics. Water Res. 43 (18), 4665–4675. https://doi.org/10.1016/j.watres.2009.07.021.

Cui, E.P., Wu, Y., Jiao, Y.A., Zuo, Y.R., Rensing, C., Chen, H., 2017. The behavior of antibiotic resistance genes and arsenic influenced by biochar during different manure composting. Environ. Sci. Pollut. R. 24 (16), 14484–14490. https://doi.org/10.1007/s11356-017-9028-z.

Czekała, W., Dach, J., Janczak, D., Smurzyńska, A., Kwiatkowska, A., Kozłowski, K., 2016. Influence of maize straw content with sewage sludge on composting process. J. Water Land Devel. 30, 43–49. https://doi.org/10.1515/jwld-2016-0020.

Eklind, Y., Kirchmann, H., 2000. Composting and storage of organic household waste with different litter amendments. II: nitrogen turnover and losses. Bioresour. Technol. 74 (2), 125–133. https://doi.org/10.1016/S0960-8524(00)00005-5.

Elwell, D.L., Keener, H.M., Hansen, R.C., 1996. Controlled, High Rate Composting of Mixtures of Food Residuals, Yard Trimmings and Chicken Manure. Compost Sci Util. 4 (1), 6–15. https://doi.org/10.1080/1065657X.1996.10701814.

Guo, R., Li, G., Jiang, T., Schuchardt, F., Chen, T., Zhao, Y., Shen, Y., 2012. Effect of aeration rate, C/N ratio and moisture content on the stability and maturity of compost. Bioresour. Technol. 112 (58), 171–178. https://doi.org/10.1016/j.biortech.2012.02.099.

He, X., Xi, B., Wei, Z., Guo, X., Li, M., An, D., Liu, H., 2011. Spectroscopic characterization of water extractable organic matter during composting of municipal solid waste. Chemosphere 82 (4), 541–548. https://doi.org/10.1016/j.chemosphere.2010.10.057.

Heerden, I.V., Cronjé, C., Swart, S.H., Kotzé, J.M., 2002. Microbial, chemical and physical aspects of citrus waste composting. Bioresour. Technol. 81 (1), 71–76. https://doi.org/10.1016/S0960-8524(01)00058-x.

Huang, C., Zeng, G.M., Huang, D.L., Lai, C., Xu, P., Zhang, C., Cheng, M., Wan, J., Hu, L., Zhang, Y., 2017. Effect of Phanerochaete chrysosporium inoculation on bacterial community and metal stabilization in lead-contaminated agricultural waste composting. Bioresour. Technol. 243, 294–303. https://doi.org/10.1016/j.biortech.2017.06.124.

Jimenz, E.I., Garcia, V.P., 1992. Determination of maturity indices for city refuse composts. Agr. Ecosyst Environ. 38, 331–343. https://doi.org/10.1016/0167-8809(92)90154-4.

Huang, J., Yang, Z.H., Zeng, G.M., Wang, H.L., Yan, J.W., Xu, H.Y., Gou, C.L., 2015. A novel approach for improving the drying behavior of sludge by the appropriate foaming pretreatment. Water Res. 68, 667–679. https://doi.org/10.1016/j.watres.2014.10.036.

Külcü, R., Yaldiz, O., 2014. The composting of agricultural wastes and the new parameter for the assessment of the process. Ecol Eng. 69, 220–225. https://doi.org/10.1016/j.ecoleng.2014.03.097.

Karak, T., Bhattacharyya, P., Paul, R.K., 2014. Assessment of Co-Compost Quality by Physico-Chemical and Exploratory Data Analysis. Clean-Soil Air Water 42 (6), 836–848. https://doi.org/10.1002/clen.201200143.

Lau, A.K., Lo, K.V., Liao, P.H., Yu, J.C., 1992. Aeration experiments for swine waste composting. Bioresour. Technol. 41 (2), 145–152. https://doi.org/10.1016/0960-8524(92)90185-Z.

Zhang, Lihua, Zeng, Guangming, Zhang, Jiachao, Chen, Yaoning, Yu, Man, Lu, Lunhui, Li, Hui, Zhu, Yuan, Yuan, Yujie, Huang, Aizhi, He, Ling, 2015. Response of denitrifying genes coding for nitrite (nirK or nirS) and nitrous oxide (nosZ) reductases to different physico-chemical parameters during agricultural waste composting. Appl Microbiol Biotechnol 99 (9), 4059–4070 http://link.springer.com/10.1007/s00253-014-6293-3. https://doi.org/10.1007/s00253-014-6293-3.

Liu, J., Zhang, X., Wang, H., Hui, X., Wang, Z., Qiu, W., 2018. Long-term nitrogen fertilization impacts soil fungal and bacterial community structures in a dryland soil of Loess Plateau in China. J. Soils Sedim. 18 (4), 1632–1640. https://doi.org/10.1007/s11368-017-1862-6.

Liu, L., Wang, S.Q., 2018. Succession and diversity of microorganisms and their association with physicochemical properties during green waste thermophilic composting. Waste Manage. 73, 101–112. https://doi.org/10.1016/j.wasman.2017.12.026.

Mao, H., Lv, Z.Y., Sun, H.D., Li, R.H., Zhai, B.N., Wang, Z.H., Awasthi, M.K., Wang, Q., Zhou, L., 2018. Improvement of biochar and bacterial powder addition on gaseous emission and bacterial community in pig manure compost. Bioresour. Technol. 258, 195–202. https://doi.org/10.1016/j.biortech.2018.02.082.

Mathur, S.P., 1991. Composting processes. Bioconvers. Waste Mater. Ind. Prod., 147–183 https://doi.org/10.1007/978-1-4615-5821-7_4.

Meng, L., Zhang, S., Gong, H., Zhang, X., Wu, C., Li, W., 2018. Improving sewage sludge composting by addition of spent mushroom substrate and sucrose. Bioresour. Technol. 253, 197–203. https://doi.org/10.1016/j.biortech.2018.01.015.

Pandey, S., Singh, S., Yadav, A.N., Nain, L., Saxena, A.K., 2013. Phylogenetic Diversity and Characterization of Novel and Efficient Cellulase Producing Bacterial Isolates from Various Extreme Environments. Biosci Biotech Bioch. 77, 1474–1480. https://doi.org/10.1271/bbb.130121.

Petiot, C., de Guardia, A., 2004. Composting in a Laboratory Reactor: A Review. Compost Sci Util. 12 (1), 69–79. https://doi.org/10.1080/1065657X.2004.10702160.

Petric, I., Šestan, A., Šestan, I., 2009. Influence of initial moisture content on the composting of poultry manure with wheat straw. Biosyst. Eng. 104 (1), 125–134. https://doi.org/10.1016/j.biosystemseng.2009.06.007.

Qian, X., Sun, W., Gu, J., Wang, X.J., Sun, J.J., Yin, Y.N., Duan, M.L., 2016. Variable effects of oxytetracycline on antibiotic resistance gene abundance and the bacterial community during aerobic composting of cow manure. J. Hazard. Mater. 315, 61–69. https://doi.org/10.1016/j.jhazmat.2016.05.002.

Rawat, I., Suthar, S., 2014. Composting of Tropical Toxic Weed Lantana camera L. Biomass and Its Suitability for Agronomic Applications. Compost. Sci. Util. 22 (3), 105–115. https://doi.org/10.1080/1065657X.2014.895455.

Reyes-Torres, M., Oviedo-Ocana, E.R., Dominguez, I., Komilis, D., Sanchez, A., 2018. A systematic review on the composting of green waste: Feedstock quality and optimization strategies. Waste Manage. 77, 486–499. https://doi.org/10.1016/j.wasman.2018.04.037.

Said-Pullicino, D., Erriquens, F.G., Gigliotti, G., 2007. Changes in the chemical characteristics of water-extractable organic matter during composting and their influence on compost stability and maturity. Bioresour. Technol. 98 (9), 1822–1831. https://doi.org/10.1016/j.biortech.2006.06.018.

Tang, Z., Yu, G., Liu, D., Xu, D., Shen, Q., 2011. Different analysis techniques for fluorescence excitation–emission matrix spectroscopy to assess compost maturity. Chemosphere 82 (8), 1202–1208. https://doi.org/10.1016/j.chemosphere.2010.11.032.

Wang, X., Selvam, A., Wong, J.W.C., 2016. Influence of lime on struvite formation and nitrogen conservation during food waste composting. Bioresour. Technol. 217, 227–232. https://doi.org/10.1016/j.biortech.2016.02.117.

Wu, C., Li, W., Wang, K., Li, Y., 2015. Usage of pumice as bulking agent in sewage sludge composting. Bioresour. Technol. 190, 516–521. https://doi.org/10.1016/j.biortech.2015.03.104.

Van der Wurff, A.W.G., Fuchs, J.G., Raviv, M., Termorshuizen, A.J., 2016. Handbook for composting and compost use in organic horticulture. BioGreenhouse COST Action FA 1105. https://doi.org/10.18174/375218.

Xi, B., He, X., Dang, Q., Yang, T., Li, M., Wang, X., Li, D., Tang, J., 2015. Effect of multi-stage inoculation on the bacterial and fungal community structure during organic municipal solid wastes composting. Bioresour. Technol. 196, 399–405. https://doi.org/10.1016/j.biortech.2015.07.069.

Xu, R., Yang, Z.-H., Zheng, Y., Zhang, H.-B., Liu, J.-B., Xiong, W.-P., Zhang, Y.-R., Ahmad, K., 2017. Depth-resolved microbial community analyses in the anaerobic co-digester of dewatered sewage sludge with food waste. Bioresour. Technol. 244, 824–835. https://doi.org/10.1016/j.biortech.2017.07.056.

Yin, Y., Jie, G., Xiaojuan, W., Wen, S., Kaiyu, Z., Wei, S., Xin, Z., Yajun, Z., Haichao, L., 2017. Effects of Copper Addition on Copper Resistance, Antibiotic Resistance Genes, and intl1 during Swine Manure Composting. Front. Microbiol. 8, 344. https://doi.org/10.3389/fmicb.2017.00344.

Yuan, J., Chadwick, D., Zhang, D.F., Li, G.X., Chen, S.L., Luo, W.H., Du, L.L., He, S.Z., Peng, S.P., 2016. Effects of aeration rate on maturity and gaseous emissions during sewage sludge composting. Waste Manage. 56, 403–410. https://doi.org/10.1016/j.wasman.2016.07.017.

Zhang, D.Q., He, P.-J., Jin, T.-F., Shao, L.-M., 2008. Bio-drying of municipal solid waste with high water content by aeration procedures regulation and inoculation. Bioresour. Technol. 99 (18), 8796–8802. https://doi.org/10.1016/j.biortech.2008.04.046.

Zhang, J., Zeng, G., Chen, Y., Huang, H., 2011. Effects of physico-chemical parameters on the bacterial and fungal communities during agricultural waste composting. Bioresour. Technol. 102 (3), 2950–2956. https://doi.org/10.1016/j.biortech.2010.11.089.

Zhang, J.N., Lu, F., Shao, L.M., He, P.J., 2014. The use of biochar-amended composting to improve the humification and degradation of sewage sludge. Bioresour. Technol. 168, 252–258. https://doi.org/10.1016/j.biortech.2014.02.080.

Zhang, J.Y., Chen, M.X., Sui, Q.W., Tong, J., Jiang, C., Lu, X.T., Zhang, Y.X., Wei, Y.S., 2016. Impacts of addition of natural zeolite or a nitrification inhibitor on antibiotic resistance genes during sludge composting. Water Res. 91, 339–349. https://doi.org/10.1016/j.watres.2016.01.010.

Zverlov, V., Mahr, S., Riedel, K., Bronnenmeier, K., 1998. Properties and gene structure of a bifunctional cellulolytic enzyme (CelA) from the extreme thermophile 'Anaerocellum thermophilum' with separate glycosyl hydrolase family 9 and 48 catalytic domains. Microbiology 144 (2), 457–465. https://doi.org/10.1099/00221287-144-2-457.